

Content from this work may be used under the terms of the CC BY 3.0 licence (© 2018). Any distribution of this work must maintain attribution to the author(s), title of the work, publisher, and DOI.

# ESRF DOUBLE CRYSTAL MONOCHROMATOR PROTOTYPE PROJECT

R. Baker, D. Baboulin, R. Barrett, P. Bernard, G. Berruyer, J. Bonnefoy, M. Brendike, P. Brumund, Y. Dabin, L. Ducotté, H. Gonzalez, G. Malandrino, P. Marion, O. Mathon, T. Roth, R. Tucoulou, European Synchrotron Radiation Facility, 38043 Grenoble, France

## Abstract

Spectroscopy beamlines at the ESRF are equipped with a generic model of double crystal monochromator (DCM), originally acquired in the 1990's. After over 20 years of continuous service, their conception, although pioneering at that time, can no longer meet the challenge of present and future scientific goals in terms of position and angular stability, thermal stability, cooling system, vibration, control and feedback, particularly in view of the ESRF - EBS upgrade.

Considering the above issues, a feasibility phase was launched to develop a prototype DCM dedicated to future spectroscopy applications at the ESRF. Specifications - derived from expected performance of the EBS upgrade and scientific objectives - are extremely challenging, especially in terms of mechanical and thermal stability and impose the adoption of several innovative design strategies. The prototype is currently in the assembly phase and tests of the complete system are planned before the end of 2018.

This article gives an overview of the DCM prototype project including specifications, major design options implemented and various validated concepts. Current project status and first test results are also presented.

## INTRODUCTION & SPECIFICATIONS

Beamlines applying experimental techniques such as X-ray Absorption Spectroscopy (XAS) in the tender to hard X-ray energy range (>2keV) are among the most demanding applications for monochromator systems. Typically such beamlines use fixed-exit double-crystal monochromators which permit scanning of the X-ray beam energy without realignment of the downstream optical components or sample. Achieving the required stability and repeatability of such devices both in terms of beam trajectory and selected photon energy is particularly challenging. This difficulty is accentuated by the progressive improvement of source and focusing optic quality as well as the challenges of management of the absorbed X-ray power which have meant that the monochromator can often be a key component limiting beamline performance.

Table 1 shows the critical target specifications for a new ESRF DCM. The values are derived from typical ESRF beamline geometries, the upgraded EBS source characteristics and the stability and precision of the energy selection. The overall specifications are particularly demanding and cannot be met by currently available devices. Consequently a new, vertically-deflecting DCM has been designed which is intended to replace ageing devices on several ESRF spectroscopy beamlines.

Table 1: Summary of Critical Specifications

Crystal parallelism	Units	Value
Pitch for $\Delta$ Bragg $<1^\circ$	nrad fwhm	15
Pitch for $\Delta$ Bragg $<5^\circ$	nrad fwhm	30
Pitch for $\Delta$ Bragg $<20^\circ$	nrad fwhm	75
Bragg angle	Units	Value
Precision	$\mu$ rad	2 - 5
Bidirectional repeatability	$\mu$ rad fwhm	25
Unidirectional repeatability	$\mu$ rad fwhm	0.2

Figure 1 indicates the 3 stage design philosophy behind the DCM concept: a strong user request is for the DCM to continue functioning, albeit in a “downgraded mode” in the case of failure of the correction and feedback loops. Every effort has therefore been made at the design stage to attain 0.1 - 0.3 $\mu$ rad/° crystal parallelism in this mode (A). Repeatable errors can be corrected after characterisation (B) and ultimate performance is achieved by using the real time control system (C).

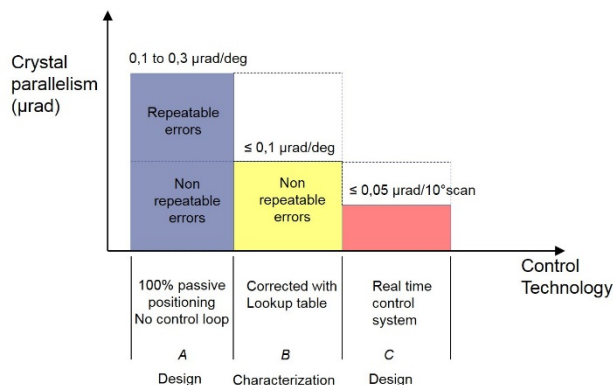


Figure 1: ESRF DCM design philosophy.

## ARCHITECTURE

Several architecture options have been evaluated:

- Cantilever cage concept
- Cantilever or split bearing cages, all in vacuum
- Split bearing and drum cage concept

Advantages and drawbacks were established for each solution, but the cantilever design was favoured, firstly due to the numerous possible identified areas of improvement over the existing concept and secondly, because the six ESRF DCMs are due for replacement and

overall architecture and crystal geometry had to be considered within certain boundary conditions imposed by existing installations.

To optimize stability there is considerable incentive to reduce the number and stroke of crystal translations required to maintain fixed exit and therefore to reduce the beam offset between the incoming and outgoing X-rays. The ESRF DCM adopts a maximum of 2 crystal pairs, fixed 1st crystals, 200mm long 2nd crystals requiring only 1 linear translation to ensure fixed exit and a 10mm downwards deflection of the exit beam.

## CONCEPTUAL DESIGN

The project has been divided into 2 main sub projects: “Bragg axis” and “Crystal cage” as shown in figure 2. Sub-division at this level does not compromise the integrated design approach of the overall device and provides straightforward pathways for re-use or modification of the two sub-assemblies for future requirements.

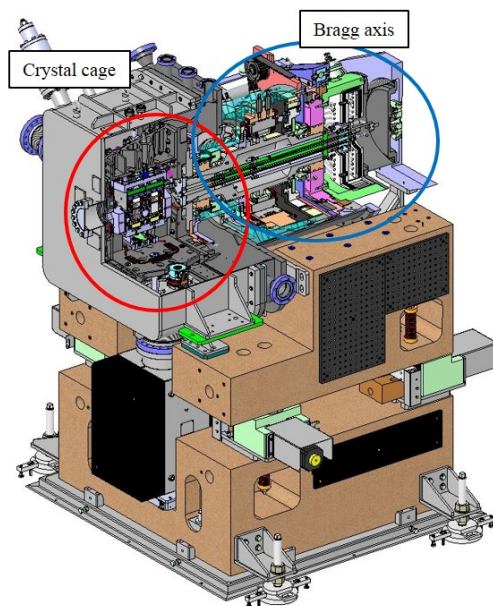


Figure 2: ESRF DCM prototype project structure.

## BRAGG AXIS

The “Bragg axis” defines all components behind the crystal cage. This includes the Bragg shaft and bearings, the Bragg motor and ex – vacuum encoder, the cryogenic feeder line management system, all ex – vacuum displacements and the main support structure.

### *Bragg drive motor*

Most current ESRF monochromators use an external, rear mounted stepper motor and reduction gears (worm wheel, gearbox...) for the Bragg drive.

More recently, we have seen DCMs exploiting “direct drive torque motors”:- a type of brushless permanent-magnet synchronous motor, with the payload directly connected to the rotor, thus using no additional transmission elements. The frameless, hollow shaft architecture allows

the motor to be ideally positioned between the Bragg bearings and close to the crystals. The large number of poles ensures the angular resolution required.

Table 2 compares the 2 drive techniques.

Table 2: Direct Drive Torque Motor vs. Stepper Motor & Gears

Parameter	Torque Motor	Stepper & Gears
Max speed	High	Medium (ratio dependent)
Wear & maintenance	Non (non-contact)	High
Radial parasitic forces	Low	Preload dependent
Aptitude to multiple scans	Good	Limited by backlash & wear
Theoretical resolution	Limited by encoder	Smallest step size
Frictional torque sensitivity	High	Lower
Friction losses	None	Preload dependent
Backlash	N/A	Wear dependent
Heat generation	High (requires cooling)	Lower
Integration	Simple (frameless, hollow shaft)	Complex (gearing or end drive)

Given the numerous advantages of the direct drive motor, the ESRF DCM prototype has been manufactured with this drive option. The ESRF has previous experience of controlling similar motors for applications other than monochromators.

The only identified drawbacks are higher thermal load, minimized by ESRF designed cooling and thermal insulation, and higher sensitivity to torque variation, managed by careful balancing of rotating parts and counterweights.

### *Bragg bearings*

The two (contradictory) principal concerns in guiding the Bragg angle axis are radial stiffness and low frictional torque. Minor guiding errors can be corrected by fine tuning of the second crystal position whereas poor radial stiffness will degrade stability and is far more complex (or impossible) to correct.

The consequence of frictional torque is the limitation of the theoretical minimum angular step size, due to the “stick – slip” effect.

Content from this work may be used under the terms of the CC BY 3.0 licence (© 2018). Any distribution of this work must maintain attribution to the author(s), title of the work, publisher, and DOI.

Low frictional torque is generally the main motivation for specifying air bearings. However, the radial stiffness of air bearings is significantly lower than that of angular contact bearings. Table 3 compares the two bearing types.

Table 3: Comparison Between Air and Angular Contact Bearings

Parameter	Air	Angular contact
<i>Typical values, geometry dependent</i>		
Frictional torque	None	2Nm (depends on axial preload)
Runout	25nm	2 $\mu$ m
Wobble	0.1 $\mu$ rad	5 - 10 $\mu$ rad
Radial stiffness	350N/ $\mu$ m	2000N/ $\mu$ m

Radial stiffness being the primary concern in the choice of Bragg shaft bearings, the ESRF DCM prototype was manufactured using two pairs of angular contact bearings in “X” configuration. The bearing arrangement is inspired from established precision spindle geometry and axial preload is optimised for the highest possible radial stiffness whilst maintaining acceptable frictional torque.

### Bragg Encoder

Specified absolute angular precision on the Bragg angle is 2 – 5 $\mu$ rad, and angular stability required is 15nrad, even when scanning, which defines an upper limit for encoder resolution.

To guarantee this level of performance, the encoder must be placed as close as possible to the crystals. This argues for the integration of an absolute encoder to the crystal plate, inside the vacuum vessel. The most suitable commercially available option is the Renishaw absolute encoder, providing 1.45nrad resolution with 32 bits encoding.

There is concern over the lifetime of the encoder read heads positioned where they are likely to be exposed to scattered radiation. Two solutions have been deployed:

Position the read heads behind the main crystal plate, where the sensitive electronics will be out of direct line of site of primary scattering and will benefit from radiation attenuation afforded by the main crystal plate. Local shielding is also implemented close to the read heads.

Integrate a second, identical encoder on the air side of the Bragg axis, as close as possible to the crystals. This encoder will be more efficiently protected from radiation and when implemented in parallel with the in-vacuum encoder, permits evaluation of the angular error induced by possible Bragg shaft twist and provides backup in the event of in-vacuum encoder failure.

### Cryogenic Feeder Line Management

Most DCMs at the ESRF are subject to absorbed power densities which can attain hundreds of W/mm<sup>2</sup>, requiring cryogenic crystal cooling. LN<sub>2</sub> feeder lines must enter the vacuum environment at a fixed point and follow the movement of the Bragg axis during scans (see Fig. 3).

It has been demonstrated that up to 85% of the total inertia seen by the Bragg drive motor is due to the displacement of these feeder lines. This is a severe performance

limitation, especially when using direct drive motors, for which torque should be kept as constant as possible.

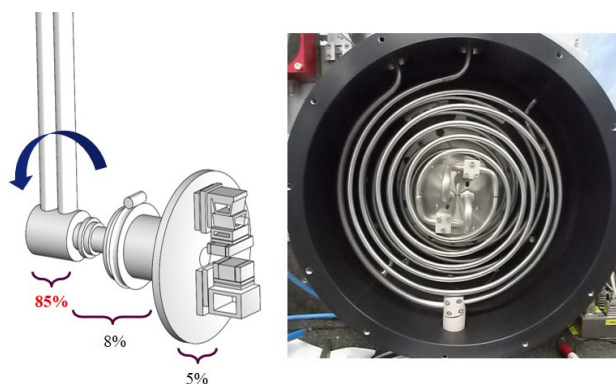


Figure 3: Feeder line management.

Hence there is a strong case for a well-balanced rotating mass and fixed feeder lines which do not perturb Bragg displacement during scanning. A novel deformable spiral tube system has been designed, supplying LN<sub>2</sub> to the crystals for cooling and thermally stabilized water to critical elements to ensure dimensional stability. The coils deform during scanning, allowing +/- 10 degrees angular displacement of the Bragg axis while the feeder lines remain fixed. For larger displacements (between scans), a stepping motor drive synchronised to the Bragg torque motor guides the external LN<sub>2</sub> feeder lines over the required angle.

### CRYSTAL CAGE

The “crystal cage” defines all components beyond the end of the Bragg axis. This includes the crystals themselves, their cooling system, alignment and displacement mechanics, the online metrology system, the support structure (plateau) and a conical interface to the Bragg shaft.

#### Plateau and Cone

To guarantee minimum deformation over the full scan range, a high stiffness plateau is mandatory. Crystal parallelism per degree of Bragg scan in the non-mechanics-assisted mode (A) is defined as  $\Delta\Theta/\Theta = 0.3 \mu\text{rad}/\text{deg}$ . This is then the target for stiffness optimization processes for all static components.

In addition, the plateau structure needs to be thermally stable despite heat loads caused by photon scattering. From the first design calculations, temperature differences of 2.7K provoke parallelism errors of up to  $\Delta\Theta = -4.81 \mu\text{rad}$  and  $\Delta\phi = 36.81 \mu\text{rad}$ . These calculations reveal the necessity to thermally control the structure.

The plateau structure was optimized in a design-calculation loop to identify lower stiffness zones and to determine deformation of the cage under gravity when loaded with the various component masses (see figure 4).

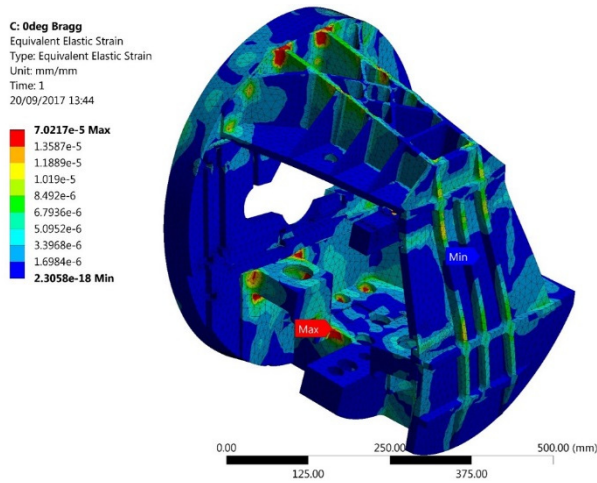


Figure 4: Plateau FEA - strain under gravity load

The structure is composed of four parts using 7075 aluminium alloy for high conductivity and good machinability. It integrates a water circuit to thermalize the structure, reducing temperature gradients.

### Crystal Clamping and Cooling

The ESRF DCM comprises two pairs of crystals in an innovative assembly (see figure 5).

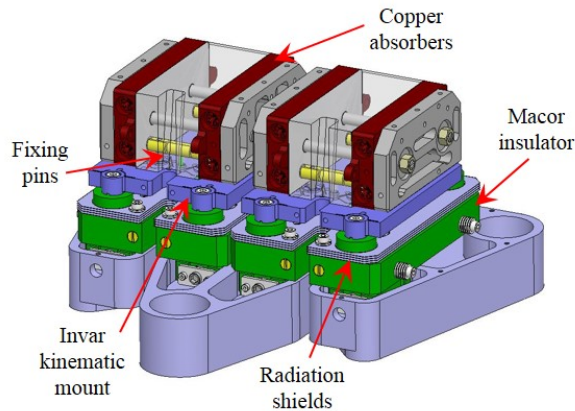


Figure 5: 1st crystal clamping setup.

Silicon crystals are fixed to an Invar plate in order to minimize differential expansion. Further, these plates integrate flexural kinematic mounts to reduce resulting forces on the crystals due to differential thermal expansion. Fixation pins traversing the crystals and screws from the bottom fix the crystals to the Invar plates. Copper absorbers are clamped to the crystal sides to extract the absorbed power.

Dynamic measurements of the assembly confirm high stiffness: a first Eigen mode of over 390Hz. Optical measurements were performed to assess relative deformation of the crystal due to clamping of the cooling blocks. Data was taken at 2 and 4 bars clamping pressure: a maximum relative P-V deformation along the meridional axis of 12.55nm was observed for 4 bars, with a resulting radius of curvature of  $\approx 50$ km.

Both crystal pairs are directly cooled. Finned channels through the 1<sup>st</sup> crystal cooling blocks optimise heat exchange. The second crystal set is cooled in series with the 1<sup>st</sup> and future developments should allow improved thermal matching between the 2 crystals.

### Fastjack

The Fastjack is a high precision linear actuator integrated to the plateau in tripod configuration to position the 2<sup>nd</sup> crystal. Three Fastjacks will operate from the horizontal plane ( $\Theta_{\text{Bragg}} = 80\text{deg}$ ) to the vertical plane ( $\Theta_{\text{Bragg}} = 2\text{deg}$ ).

The 2 stage actuator comprises a long stroke driven by a stepper motor, and a 2nd stage for fast position errors correction using a piezo actuator. The stepper actuator is specified for a minimum incremental motion (MIM) of 100nm; the piezo actuator and its regulation loop should achieve a MIM of a few nanometres with an actuation bandwidth of 100Hz. Careful design optimisation has been performed for both maximum stiffness and nano-positioning capabilities. Long travel displacement is ensured by a precision screw / nut and guiding by a ball bush guide.

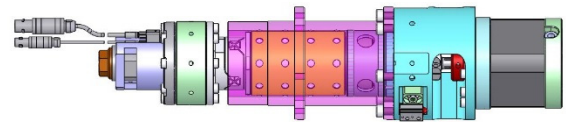


Figure 6: ESRF Fastjack.

Together with the DCM embedded metrology system, the 3 actuators will optimise position repeatability the stability of the 2nd crystals. During a scan or at fixed energy, repeatability and stability of around 15nrad implies about 5nm displacement at the actuator level.

The Fastjack is capable of a stroke of 30mm, a speed of up to 8mm/s, acceleration rate of 100mm/s<sup>2</sup>, and an actuation force above 100N. Specified lifetime is  $\sim 10^7$  cycles under UHV conditions. Water-cooling is also integrated.

### Online Metrology

To maintain crystal parallelism to within defined specifications over the entire scan range is perhaps the most challenging aspect of the entire DCM design: intrinsic dynamic behaviour and thermal gradients make it impossible to envisage such stability uniquely through passive mechanical design. Based upon the severity of the specifications for parallelism stability, an online metrology system, using multiple radiation resistant Fabry - Perot interferometer heads, has been integrated to monitor the angular drifts of the 2nd crystal and allow correction of its position in real time.

Overlap of the crystals at higher Bragg angles severely restricts accessibility to the diffracting surface for positional metrology and direct exposure to high levels of scattered radiation for prolonged periods may limit component lifetime. Consequently, the interferometer beams will target the rear face of the crystals. This is already a significant challenge and a major improvement over existing systems.

Content from this work may be used under the terms of the CC BY 3.0 licence (© 2018). Any distribution of this work must maintain attribution to the author(s), title of the work, publisher, and DOI.

Parallelism between the crystalline planes and the rear of the crystal is supposed fixed.

A dedicated metrology frame carries 3 interferometers to monitor pitch, roll and fixed exit translation of each of the 2nd crystals. The position of the 1st crystals - directly attached to the Bragg axis - is considered fixed. However, on the prototype, this will be monitored, as will any possible differential displacement of the metrology frame itself. Thus, a total of 15 interferometers are deployed (3 for each crystal and 3 for the metrology frame). Figure 7 shows the schematic layout.

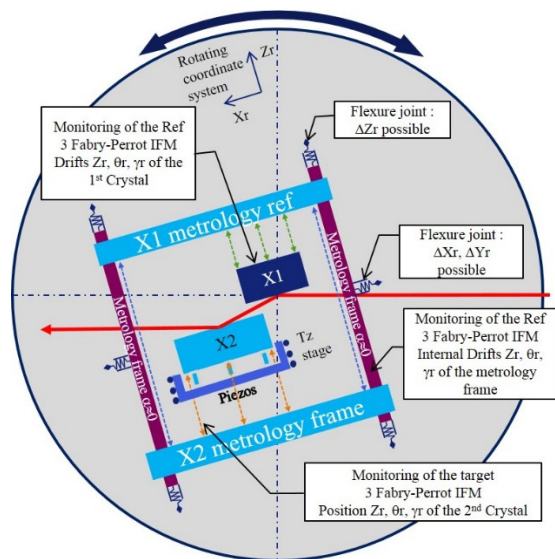


Figure 7: Online crystal metrology schematic layout.

As requested, the DCM can continue to operate in a degraded performance mode in the event of failure of the online metrology system.

## FIRST RESULTS

### Bragg Axis

By using the torque motor with a linear controller and the in-air position encoder, first tests give a minimal incremental motion and a repeatability of  $0.25 \mu\text{rad}$ . This is still above final specifications, but performance is expected to improve following further tests using an optimized control algorithm (see Figure 8).

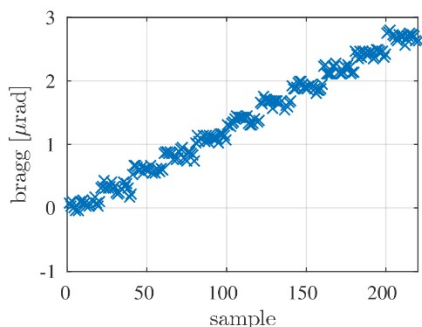


Figure 8: Bragg axis resolution in air.

### Fastjack

The first tests of the Fastjack show promising results. In-air tests with a load of 5kg show a minimal incremental motion of about 15nm over a stroke of 30mm. Further, the dynamic performance of the actuator was pushed to a bandwidth of over 100Hz by using advanced control algorithms. This was achieved using a feedback loop consisting of the online metrology system and a real-time controller (see Figure 9).

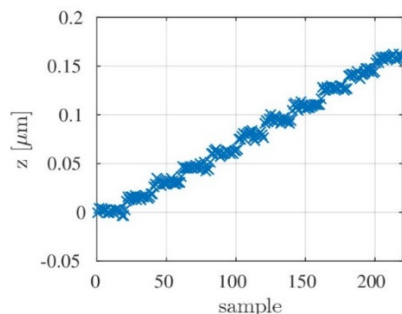


Figure 9: Fastjack resolution in air.

At the time of writing, the measurements are limited by the in-air performance of our reference Interferometer, which shows a noise level of about 10nm. By moving the setup from the in-air test bench to the vacuum chamber of the DCM, a further performance improvement is expected.

## CONCLUSION

Derived from the expected performance of the ESRF EBS, specifications for a new generation DCM are extremely challenging and impose exhaustive reconsideration and optimisation of every identified weakness in current designs.

This has been the driving philosophy behind the ESRF DCM prototype project and following a comprehensive design phase, manufacture is now complete and assembly, alignment and initial metrology are being performed in house. First results from off-line lab metrology are encouraging and installation and commissioning on ESRF's X-ray microscopy beamline ID21 are foreseen before the 18 month EBS shutdown (December 2018 – mid 2020).

## ACKNOWLEDGEMENTS

The authors would like to thank all ESRF staff involved in the DCM prototype project, including:

H.P. van der Kleij, M. Lesourd, L. Rousset, R. Grivelet, P. Voisin, A. Vivo, M. Cotte, M. Salomé, K. Martel, D. Bugnazet, R. Hino, K. Amraoui